

Application of machine learning technique in predicting condensation heat transfer coefficient and droplet entrainment rate

Jee Min Yoo¹, Dong Hyun Lee¹, Dong Jin Hong² and Jae Jun Jeong^{1*}

¹Department of Mechanical Engineering, ²Department of Computer Engineering, Pusan National University
2, Busandaehak-ro, 63 beon-gil, Geumjeong-gu, Busan, 16241, Republic of Korea

*Corresponding author: jjjeong@pusan.ac.kr

1. Introduction

Machine learning technique is a useful method for constructing models that infer specific answers or interpret complex systems based on data including input parameters and output. Due to this characteristic, recently, many researches have been actively conducted to develop a model that predicts thermal-hydraulic phenomena using machine learning [1-10].

In general, thermal-hydraulic models are developed by analyzing the relationship between key parameters and hundreds or thousands of experimental data. At this time, machine learning can be effectively used in the step of finding the relationship between key parameters and data. This is because a machine learning method is specialized in finding complex relationships between data. However, hundreds or thousands of experimental data are a small quantity to be used as training data for machine learning. If the amount of data is small, the machine learning model may be overfitting, resulting in low generalization performance. In this study, the problem of an insufficient amount of data was solved through pseudo data produced by using the existing thermal-hydraulic correlations [4]. Through several studies [4, 11-15], it has been confirmed that a model with a deep neural network structure exhibits superior problem-solving ability. Therefore, to build a machine learning model with good prediction performance, DenseNet [15], the latest deep learning algorithm based on convolution neural network (CNN), was applied for data training.

This study is a step to confirm the applicability of machine learning techniques using pseudo data to predict thermal-hydraulic phenomena. Two phenomena were used as confirmation objects. The first one is condensation heat transfer occurring in the passive containment cooling system (PCCS), and the second one is a phenomenon in which droplets are separated from the liquid film under the annular-mist flow condition formed in the reactor core of the reflood phase. Experimental data and existing correlations for the two phenomena were collected, and each correlation was evaluated using the experimental data. Based on the evaluation results, pseudo data to be used for training was generated. The machine learning model trained on these data was assessed using the collected experimental data.

2. Experimental data and existing correlations

2.1 Condensation heat transfer

In design basis accidents such as a loss of coolant accident (LOCA) or a main steam line break (MSLB) accident, high-temperature steam is released into the containment filled with atmospheric pressure air. This increases the pressure and temperature inside the containment. The PCCS is a safety system to effectively reduce the temperature and pressure inside the containment. The PCCS consists of several tube heat exchangers. In the accidents, the tube heat exchangers remove heat from the air-steam mixture through natural convection heat transfer and condensation heat transfer. At this time, air, which is a noncondensable gas (NCG), interferes with condensation, which has a great influence on the PCCS performance.

To investigate the PCCS performance, condensation heat transfer experiments using a single tube under natural convection have been performed [16-25]. Table I shows the test conditions of each experiment. Most researchers have presented a correlation to predict the condensation heat transfer coefficient (HTC) based on their own experimental data: Dehbi[16], Liu[17], Su[19,20], Lee[21], Jang[23], Kim [24], Kang [25], Fan [26]. There is also a well-known Dehbi's semi-empirical model [27]. The model assessment was performed based on the experimental data in Table I to identify the prediction performance of the existing correlations. Table II shows the mean absolute error (MAE) of each correlation for 10 experiments.

$$MAE = \frac{1}{n} \sum_{i=1}^n \frac{C_i - M_i}{M_i}, \quad (1)$$

where n , C_i , and M_i are the number of data, calculated value, and measured value, respectively. As a result of the MAE comparison, the correlations predicted well an experiment within the application range but did not have good prediction results for all experiments.

2.2 Droplet entrainment

Various two-phase flows are formed in the reactor core in the reflood phase of a large-break LOCA. Among them, in the annular-mist flow, droplets are generated by the interfacial friction between high-velocity steam and liquid film. The generated droplets contribute greatly to cooling the core through wall heat transfer and interfacial heat transfer.

Table I : Test conditions of the condensation heat transfer experiments

Exp.	Tube diameter (m)	Tube length (m)	Total pressure (bar)	NCG mass fraction	Wall subcooling (K)	No. of data
Dehbi [16]	0.038	3.5	1.5-4.5	0.25-0.91	10-50	107
Liu [17]	0.04	2.0	2.5-4.6	0.17-0.75	3.8-26.8	26
Kim [18]	0.0412	0.65	4.0-20.0	0.10-0.72	50-60	72
Su [19]	0.038	2.0	2.0-6.0	0.20-0.80	27-70	145
Su [20]	0.038	2.0	4.0-6.0	0.20-0.52	13-70	19
Lee [21]	0.04	1.0	2.0-5.0	0.10-0.80	20-69	43
Fan [22]	0.0321	2.0	2.0-6.0	0.20-0.80	27-70	212
Jang [23]	0.01	1.0	2.0-5.0	0.10-0.90	18-69	20
Kim [24]	0.0215	1.0	2.0-5.0	0.10-0.80	40	39
Kang [25]	0.0215 0.0336 0.0424	1.33 1.28	2.0-6.0	0.20-0.80	16-56	195

Many air-water experiments [28-36] have been performed to investigate droplet behaviors under a vertical annular-mist flow condition. These experiments measured the mass fraction of the entrained droplet at the outlet of the test section. The entrained droplet mass fraction is determined by the droplet entrainment rate and the deposition rate. In the case of droplet deposition rate, direct measurement is possible in the experiment

by the double film extraction method, but in the case of droplet entrainment rate, it is very difficult to directly measure it in the experiment because droplet deposition and entrainment occur at the same time. Therefore, the deposition correlation was derived based on actual experimental data, but the entrainment correlation was proposed based on the estimated value from the mass balance equation.

Using the collected experimental data in Table III, the droplet entrainment correlations of Hewitt [37], Lopez de Bertodano [38], Okawa [39], and Han [40] were assessed. At this time, Okawa's deposition model [39] was used for the assessment. Table IV shows the MAE of each correlation for 10 experiments. From the table, it was confirmed that there is no correlation that gives good results for all experiments.

Table III: Test conditions of the droplet entrainment experiments

Exp.	Dia. [mm]	Pressure [bar]	Gg [kg/m ² /s]	Gl [kg/m ² /s]	No. of data
Barbosa [28]	31.8	2.0-5.2	13-56	11-330	75
Okawa [29]	5.0	1.4-7.6	86-628	89-1630	170
Whalley [30]	31.8	1.2-3.5	3-235	8-710	156
Sawant [31]	9.4	1.2-4.0	41-446	43-473	30
Fore [32]	50.8	1.0	24-44	16-69	44
Jagota [33]	25.4	2.8-4.2	41-162	47-449	27
Asali [34]	22.9 42	1.0-2.0	30-130	6-126	55
Magrini [35]	76.2	1.0-1.5	67-130	4-40	20
Hinkle [36]	12.6	2.8-6.2	52-254	103-530	27

Table II: The MAE of each condensation HTC correlation

Model \ Exp.	Dehbi [16]	Liu [17]	Su [19]	Su [20]	Dehbi [27]	Lee [21]	Fan [26]	Jang [23]	Kim [24]	Kang [25]
Dehbi [16]	0.041	0.630	0.154	0.397	0.076	0.059	0.207	0.553	0.060	0.079
Liu [17]	0.318	0.114	0.652	0.317	0.196	0.387	0.496	0.327	0.387	0.357
Kim [18]	0.109	0.585	0.303	0.739	0.147	0.641	0.571	0.609	0.643	0.519
Su [19]	0.083	1.085	0.099	0.287	0.045	0.222	0.093	0.157	0.217	0.191
Su [20]	0.233	0.098	0.176	0.044	0.170	0.451	0.096	0.354	0.446	0.353
Lee [21]	0.589	2.023	0.798	0.777	0.635	0.165	0.835	0.173	0.165	0.187
Fan [22]	0.122	0.740	0.079	0.317	0.124	0.150	0.071	0.161	0.141	0.106
Jang [23]	0.286	0.420	0.197	0.249	0.140	0.780	0.157	0.108	0.200	0.178
Kim [24]	0.089	0.776	0.096	0.264	0.124	0.107	0.131	0.194	0.080	0.087
Kang [25]	0.214	1.096	0.418	0.525	0.328	0.207	0.439	0.154	0.162	0.073
Total	0.158	0.876	0.243	0.416	0.181	0.229	0.269	0.254	0.203	0.161

Table IV: The MAE of each droplet entrainment correlation

Experiment	Droplet entrainment correlations			
	Han [40]	Okawa [39]	Hewitt [37]	Lopez [38]
Barbosa [28]	0.275	0.327	0.530	0.928
Okawa [29]	0.933	0.273	1.062	0.501
Whalley [30]	0.147	0.228	0.231	0.417
Sawant [31]	0.499	0.386	0.899	0.583
Fore [32]	0.375	0.269	0.136	0.785
Jagota [33]	0.189	0.263	0.428	0.808
Asali-22.9 [34]	0.179	0.144	0.179	0.489
Asali-42 [34]	0.338	0.356	0.224	0.632
Magrini [35]	0.130	0.310	0.231	0.217
Hinkle [36]	0.641	0.335	0.873	0.796
Total	0.527	0.291	0.675	0.626

3. Machine learning model

Machine learning technique was applied to improve the prediction for all experimental data. To prepare enough training data, pseudo data was established based on the assessment results of the existing correlations.

3.1 Pseudo data

To replace the experimental data, the pseudo data should be composed of datasets that include the test conditions of each experiment. To secure quality data, the pseudo data for each experimental range was created using a correlation that gave the smallest error for each experiment (see Tables II and IV).

The pseudo condensation HTC data was generated based on the total pressure (P_t), mass fraction of the NCG (W_{ncg}), and wall subcooling ($\Delta T_{w,sub}$) (see Table I).

$$h_{c,pd} = f_c(P_t, W_{ncg}, \Delta T_{w,sub}), \quad (2)$$

where f_c is the condensation heat transfer correlation. About 540,000 pseudo data were created in the thermal-hydraulic range of 10 experiments. The pseudo data consisted of 7 input parameters P_t , W_{ncg} , $\Delta T_{w,sub}$, tube diameter, tube length, Jakob number, and Grashof number, and an output parameter, condensation HTC.

Pseudo data for the droplet entrainment rate was generated in the same way.

$$m_{e,pd} = f_e(P, G_g, G_l), \quad (3)$$

where f_e is the droplet entrainment correlation. G_g and G_l denote gas and liquid mass flux, respectively. Based on the MAE in Table IV, about 1.3 million pseudo data were produced in the thermal-hydraulic range of 10 experiments. These data consisted of 9 input parameters hydraulic diameter, P , G_g , G_l , ρ_g , ρ_l , μ_g , μ_l , and σ , and an output parameter, the droplet entrainment rate.

The data obtained in this way were classified into training, validation, and test datasets through random sampling and applied to machine learning.

3.2 Model architecture

In a traditional neural network such as multi-layer perceptron (MLP), the order of input parameters does not affect the result because all nodes of each layer are fully connected. Because the input parameters for predicting the condensation HTC and the droplet entrainment rate have no meaning in the order, a traditional neural network composed of a fully connected layer is suitable. However, the MLP has limitations in constructing a deep network. In this paper, a machine learning model with DenseNet-based architecture [15] was applied to obtain a deep network structure. DenseNet, a CNN-based algorithm, improves prediction performance by receiving outputs of all previous layers as inputs of a subsequent layer (Fig. 1).

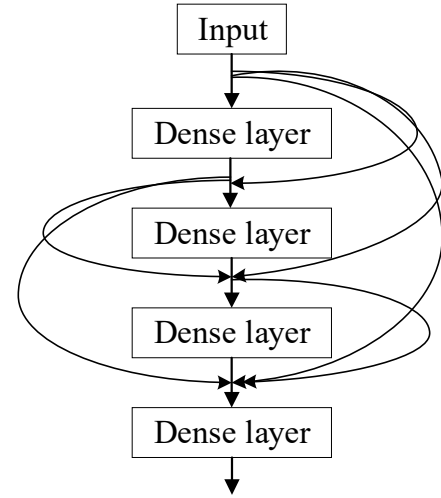


Fig. 1. Dense block in DenseNet

The machine learning model of this study consisted of the MLP for expansion of input parameters, and DenseNet, for learning the expanded inputs (Fig. 2). The CNN-based models receive data in a two-dimensional form as input and performs local operation that computes on a part of the input. Therefore, if parameters with independent information in a one-dimensional form are used as an input of DenseNet without any processing, the order of the parameters affects the learning result. Since the MLP connects all input parameters, it can be said that the output of the MLP contains all information of the input parameters. Based on this, to consider all input parameters of the pseudo data, the output obtained through the MLP was transferred to the input of DenseNet. At this time, the output of the MLP was reshaped into a two-dimensional form before entering DenseNet. And the reduction in learning performance that may occur due to local operation was complemented by concatenating three parallelized MLPs. The DenseNet structure consisted of two dense blocks. The first one had 6 dense layers, and the second one had 12 dense layers. In the last part of the model, a global average pooling and a dense operation were conducted to obtain one output (Fig. 2).

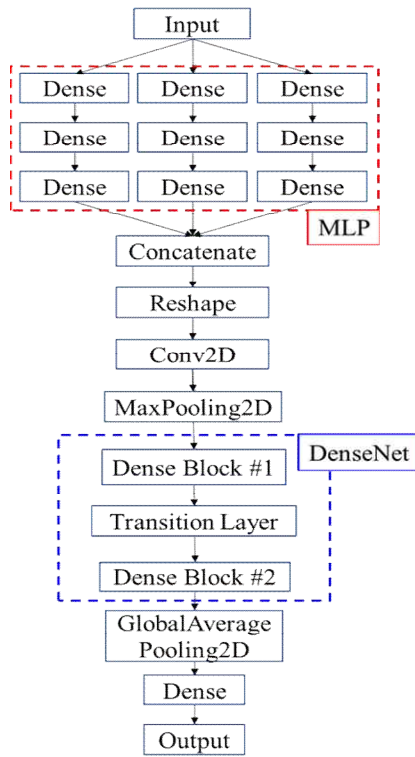


Fig. 2. Architecture of the machine learning model

3.3 Prediction results

The machine learning model was trained for each pseudo data of the condensation heat transfer and the droplet entrainment. The trained model was assessed using the experimental data in Tables I and III. First, the assessment results for the condensation HTC are presented in Table V and Fig. 3. It can be seen from Table V that the prediction performance of the machine learning model is excellent for all experimental data. The assessment results for the droplet entrainment rate are shown in Table VI and Fig. 4. Similarly, when compared with the results in Table IV, the trained model gave a small error for all experiments.

Table V: The MAE of the machine learning model for the condensation experiments

Experiment	MAE
Dehbi [16]	0.044
Liu [17]	0.117
Kim [18]	0.112
Su [19]	0.115
Su [20]	0.047
Lee [21]	0.173
Fan [22]	0.075
Jang [23]	0.112
Kim [24]	0.077
Kang [25]	0.081
Total	0.088

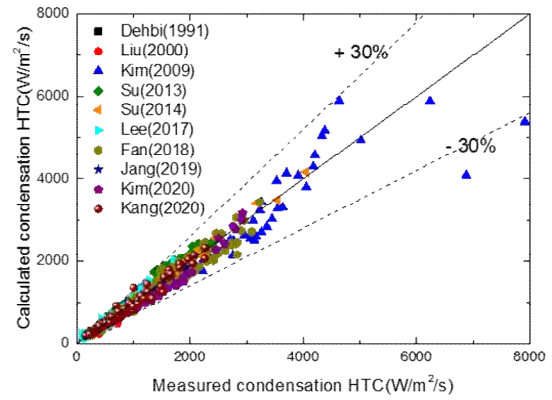


Fig. 3. Assessment result of the machine learning model for the condensation experiments

Table VI: The MAE of the machine learning model for the droplet entrainment experiments

Experiment	MAE
Barbosa [18]	0.274
Okawa [19]	0.273
Whalley [20]	0.148
Sawant [21]	0.383
Fore [22]	0.138
Jagota [23]	0.194
Asali-22.9 [24]	0.131
Asali-42 [24]	0.196
Magrini [25]	0.122
Hinkle [26]	0.332
Total	0.255

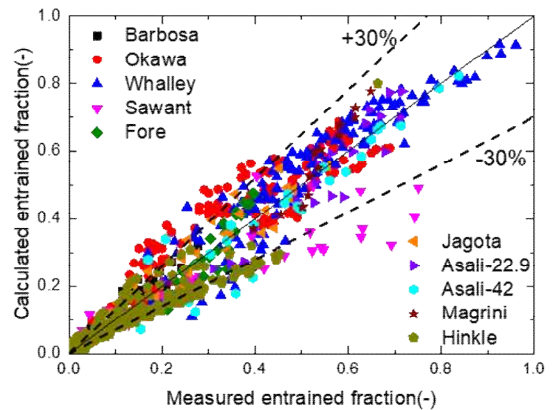


Fig. 4. Assessment result of the machine learning model for the droplet entrainment experiments

4. Conclusions

In this study, the existing correlations for the condensation heat transfer including noncondensable gas and the droplet entrainment in a vertical annular-mist flow were investigated, and they were assessed using collected experimental data. Consequently, each correlation showed satisfactory prediction results for the experiments within its application range but did not predict all experiments well. To solve this problem, a machine learning technique was applied. To obtain

sufficient training data, pseudo data was produced based on the existing correlations. And these data were trained using the latest deep learning method. The trained machine learning model was assessed using experimental data. As a result, the trained model gave good prediction results for all experimental data.

This study confirmed the applicability and feasibility of the machine learning technique for predicting thermal-hydraulic phenomena. As a future work, we plan to expand the application range of the machine learning model by adding the condensation experiments under a flat plate condition and the steam-water experiments for an annular-mist flow. The final goal is to present a new correlation through a parametric study based on the machine learning model.

Acknowledgement

This research was supported by the National Research Foundation (NRF) grant funded by the Ministry of Science, and ICT of the Korean government (Grant code 2017M2A8A4015059).

REFERENCES

- [1] L. Zhou, D. Garg, Y. Qiu, S.M. Kim, I. Mudawar, and C.R. Kharangate. Machine learning algorithms to predict flow condensation heat transfer coefficient in mini/micro-channel utilizing universal data. *International Journal of Heat and Mass Transfer*, 162, 120351, 2020.
- [2] H.M. Park, J.H. Lee, and K.D. Kim. Wall temperature prediction at critical heat flux using a machine learning model. *Annals of Nuclear Energy*, 141, 107334, 2020.
- [3] Y. Qiu, D. Garg, L. Zhou, C.R. Kharangate, S.M. Kim, and I. Mudawar. An artificial neural network model to predict mini/micro-channels saturated flow boiling heat transfer coefficient based on universal consolidated data. *International Journal of Heat and Mass Transfer*, 149, 119211, 2020.
- [4] H. Kim, J. Moon, D. Hong, E. Cha, and B. Yun. Prediction of critical heat flux for narrow rectangular channels in a steady state condition using machine learning. *Nuclear Engineering and Technology*, 2020.
- [5] W. Chang, X. Chu, A.F.B.S. Fareed, S. Pandey, J. Luo, B. Weigand, and E. Laurien. Heat transfer prediction of supercritical water with artificial neural networks. *Applied Thermal Engineering*, 131, 815-824, 2018.
- [6] A. Khosravi, J.J.G. Pabon, R.N.N. Koury, and L. Machado. Using machine learning algorithms to predict the pressure drop during evaporation of R407C. *Applied Thermal Engineering*, 133, 361-370, 2018.
- [7] G. Zhu, T. Wen, and D. Zhang. Machine learning based approach for the prediction of flow boiling/condensation heat transfer performance in mini channels with serrated fins. *International Journal of Heat and Mass Transfer*, 166, 120783, 2021.
- [8] P. Behnam, M. Faegh, M.B. Shafii, and M. Khiadani. A comparative study of various machine learning methods for performance prediction of an evaporative condenser. *International Journal of Refrigeration*, 2021.
- [9] X. Zhao, K. Shirvan, R.K. Salko, and F. Guo. On the prediction of critical heat flux using a physics-informed machine learning-aided framework. *Applied Thermal Engineering*, 164, 114540, 2020.
- [10] G.M. Hobold, and A.K. da Silva. Automatic detection of the onset of film boiling using convolutional neural networks and Bayesian statistics. *International Journal of Heat and Mass Transfer*, 134, 262-270, 2019.
- [11] K. Simonyan, and A. Zisserman. Very deep convolutional networks for large-scale image recognition. *arXiv preprint arXiv:1409.1556*, 2014.
- [12] C. Szegedy, W. Liu, Y. Jia, P. Sermanet, S. Reed, D. Anguelov, D. Erhan, V. Vanhoucke, and A. Rabinovich. Going deeper with convolutions. In *Proceedings of the IEEE conference on computer vision and pattern recognition*, p. 1-9, 2015.
- [13] K. He, X. Zhang, S. Ren, and J. Sun. Deep residual learning for image recognition. In *Proceedings of the IEEE conference on computer vision and pattern recognition*, p. 770-778, 2016.
- [14] J. Hu, L. Shen, and G. Sun. Squeeze-and-excitation networks. In *Proceedings of the IEEE conference on computer vision and pattern recognition*, p. 7132-7141, 2018.
- [15] G. Huang, Z. Liu, L. Van Der Maaten, and K.Q. Weinberger. Densely connected convolutional networks. In *Proceedings of the IEEE conference on computer vision and pattern recognition*, p. 4700-4708, 2017.
- [16] A. Dehbi, The effects of noncondensable gases on steam condensation under turbulent natural convection conditions, Doctoral dissertation, Massachusetts Institute of Technology, 1991.
- [17] H. Liu, N.E. Todreas, and M.J. Driscoll. An experimental investigation of a passive cooling unit for nuclear plant containment. *Nuclear engineering and design*, 199(3), 243-255, 2000.
- [18] J.W. Kim, Y.G. Lee, H.K. Ahn, and G.C. Park. Condensation heat transfer characteristic in the presence of noncondensable gas on natural convection at high pressure. *Nuclear Engineering and Design*, 239(4), 688-698, 2009.
- [19] J. Su, Z. Sun, G. Fan, M. Ding. Experimental study of the effect of non-condensable gases on steam condensation over a vertical tube external surface. *Nuclear Engineering and Design*, 262, 201-208, 2013.
- [20] J. Su, Z. Sun, M. Ding, and G. Fan. Analysis of experiments for the effect of noncondensable gases on steam condensation over a vertical tube external surface under low wall subcooling. *Nuclear Engineering and Design*, 278, 644-650, 2014.
- [21] Y.G. Lee, Y.J. Jang, and D.J. Choi. An experimental study of air-steam condensation on the exterior surface of a vertical tube under natural convection conditions. *International Journal of Heat and Mass Transfer*, 104, 1034-1047, 2017.
- [22] G. Fan, P. Tong, Z. Sun, and Y. Chen. Experimental study of pure steam and steam-air condensation over a vertical corrugated tube. *Progress in Nuclear Energy*, 109, 239-249, 2018.
- [23] Y.J. Jang, D.J. Choi, S. Kim, D.W. Jerng, and Y.G. Lee. Development of an empirical correlation for condensation heat transfer coefficient on a vertical tube in the presence of a noncondensable gas, *Trans. Korean Soc. Mech. Eng. B*, 42(3), p. 187-196, 2018.
- [24] U.K. Kim, J.W. Yoo, Y.J. Jang, and Y.G. Lee. Measurement of heat transfer coefficients for steam condensation on a vertical 21.5-mm-OD tube in the presence of air. *Journal of Nuclear Science and Technology*, 57(8), 905-916, 2020.
- [25] J. Kang, H. Kim, J. Bak, S.G. Lim, and B. Yun. Condensation of steam mixed with non-condensable gas on

vertical heat exchanger tubes in circumstances with free convection. *International Journal of Heat and Mass Transfer*, 169, 120925, 2021.

[26] G. Fan, P. Tong, Z. Sun, and Y. Chen. Development of a new empirical correlation for steam condensation rates in the presence of air outside vertical smooth tube. *Annals of Nuclear Energy*, 113, 139-146, 2018.

[27] A. Dehbi. A generalized correlation for steam condensation rates in the presence of air under turbulent free convection. *International Journal of Heat and Mass Transfer*, 86, 1-15, 2015.

[28] J.R. Barbosa Jr, G.F. Hewitt, G. König, and S.M. Richardson. Liquid entrainment, droplet concentration and pressure gradient at the onset of annular flow in a vertical pipe. *International Journal of Multiphase Flow*, 28(6), 943-961, 2002.

[29] T. Okawa, A. Kotani, and I. Kataoka. Experiments for liquid phase mass transfer rate in annular regime for a small vertical tube. *International Journal of Heat and Mass Transfer*, 48(3-4), 585-598, 2005.

[30] P.B. Whalley, G.F. Hewitt, and P. Hutchinson. Experimental wave and entrainment measurements in vertical annular two-phase flow. AERE-R,7521.

[31] P. Sawant, M. Ishii, and M. Mori. Droplet entrainment correlation in vertical upward co-current annular two-phase flow. *Nuclear Engineering and Design*, 238(6), 1342-1352, 2008.

[32] L.B. Fore, and A.E. Dukler. Droplet deposition and momentum transfer in annular flow. *AIChE Journal*, 41(9), 2040-2046, 1995.

[33] A.K. Jagota, E. Rhodes, and D.S. Scott. Tracer measurements in two phase annular flow to obtain interchange and entrainment. *The Canadian Journal of Chemical Engineering*, 51(2), 139-148, 1973.

[34] J.C. Asali. Entrainment in Vertical Gas-Liquid Annular Flow. Doctoral dissertation, University of Illinois at Urbana-Champaign, Urbana, Illinois, 1985.

[35] K.L. Magrini, C. Sarica, A. Al-Sarkhi, and H.Q. Zhang. Liquid entrainment in annular gas/liquid flow in inclined pipes. *SPE Journal*, 17(02), 617-630, 2012.

[36] W.D. Hinkle. A study of liquid mass transport in annular air-water flow, Doctoral dissertation, Massachusetts Institute of Technology, 1967.

[37] G.F. Hewitt, and A.H. Govan. Phenomenological modelling of non-equilibrium flows with phase change. *International journal of heat and mass transfer*, 33(2), 229-242, 1990.

[38] M.A. Lopez de Bertodano, C.S. Jan, and S.G. Beus. Annular flow entrainment rate experiment in a small vertical pipe. *Nuclear engineering and design*, 178(1), 61-70, 1997.

[39] T. Okawa, T. Kitahara, K. Yoshida, T. Matsumoto, and I. Kataoka. New entrainment rate correlation in annular two-phase flow applicable to wide range of flow condition. *International Journal of Heat and Mass Transfer*, 45(1), 87-98, 2002.

[40] K.H. Han, J.M. Yoo, B.J. Yun, and J.J. Jeong. Development of a droplet entrainment rate model for a vertical adiabatic two-phase flow. *Annals of Nuclear Energy*, 132, 181-190, 2019.